ELSEVIER

NeuroImage

www.elsevier.com/locate/ynimg
NeuroImage 31 (2006) 153 – 159

Mu rhythm (de)synchronization and EEG single-trial classification of different motor imagery tasks

G. Pfurtscheller,[a,*] C. Brunner,[a] A. Schlögl,[a] and F.H. Lopes da Silva[b]

[a]*Laboratory of Brain–Computer Interfaces, Institute for Computer Graphics and Vision, Graz University of Technology, Inffeldgasse 16a, A-8010 Graz, Austria*
[b]*Centre of Neurosciences, Swammerdam Institute for Life Sciences, University of Amsterdam, Kruislaan 320, NL-1098 SM Amsterdam, The Netherlands*

Received 23 February 2005; revised 11 November 2005; accepted 1 December 2005
Available online 27 January 2006

We studied the reactivity of EEG rhythms (mu rhythms) in association with the imagination of right hand, left hand, foot, and tongue movement with 60 EEG electrodes in nine able-bodied subjects. During hand motor imagery, the hand mu rhythm blocked or desynchronized in all subjects, whereas an enhancement of the hand area mu rhythm was observed during foot or tongue motor imagery in the majority of the subjects. The frequency of the most reactive components was 11.7 Hz ± 0.4 (mean ± SD). While the desynchronized components were broad banded and centered at 10.9 Hz ± 0.9, the synchronized components were narrow banded and displayed higher frequencies at 12.0 Hz ± 1.0. The discrimination between the four motor imagery tasks based on classification of single EEG trials improved when, in addition to event-related desynchronization (ERD), event-related synchronization (ERS) patterns were induced in at least one or two tasks. This implies that such EEG phenomena may be utilized in a multi-class brain–computer interface (BCI) operated simply by motor imagery.

Introduction

A fundamental property of a neural network is the ability of neurons to work in synchrony and to generate oscillatory activity (Lopes da Silva, 1991). One prominent group of such brain oscillations has frequencies between 9–13 Hz in man and 12–15 Hz in cat and originates in sensorimotor areas. These activities are known as "rolandic mu rhythms" or "wicket rhythms" in man (Niedermeyer, 1993; Gastaut, 1952) and sensorimotor rhythms (SMRs) in cat (Chase and Harper, 1971; Howe and Sterman, 1972).

It is well known that planning and execution of hand and/or finger movement block or desynchronize the mu rhythm (Chatrian et al., 1959), and inhibition of motor behavior synchronizes the SMR (Howe and Sterman, 1972). The importance of such an enhancement of 12- to 15-Hz oscillations for biofeedback therapy was documented already in the seventies by Sterman et al. (1974) and confirmed by Egner and Gruzelier (2001) and others. It was already demonstrated that externally paced foot and tongue movement and imagination of foot movement (Pfurtscheller and Neuper, 1994, 1997) can enhance the hand area mu rhythm, similar as observed during reading of words (Pfurtscheller, 1992), pattern vision (Koshino and Niedermeyer, 1975) or flicker stimulation (Brechet and Lecasble, 1965). This ability to suppress or enhance the amplitude of the hand area mu rhythm consciously by directing attention to different body parts or limbs is not only of interest to suppress epileptic seizures by neurofeedback therapy (Sterman et al., 1974) but also for realizing an EEG-based brain–computer interface (BCI) with motor imagery as a mental strategy (Wolpaw et al., 2002; Pfurtscheller and Neuper, 2001).

The goals of this paper are

(i) to study the inter- and intrasubject variability of event-related EEG (de)synchronization patterns (ERD/ERS) in four motor imagery tasks,
(ii) to study whether the same or different frequency components are involved in desynchronization and synchronization patterns recorded from the same cortical areas,
(iii) to report on the distinctiveness between four different motor imagery tasks when single trials are analyzed and classified, and
(iv) to provide recommendations for the realization of a multi-class BCI with improved classification accuracy.

Methods

Subjects and experimental paradigm

Six female and three male healthy right-handed subjects (mean age 26.2 years, range 21–31 years) participated in this

* Corresponding author. Fax: +43 316 873 5349.
E-mail address: pfurtscheller@tugraz.at (G. Pfurtscheller).
Available online on ScienceDirect (www.sciencedirect.com).

1053-8119/$ - see front matter © 2005 Elsevier Inc. All rights reserved.
doi:10.1016/j.neuroimage.2005.12.003

study. They sat in a comfortable armchair in an electrically shielded cabin watching a 15″ monitor from a distance of about 2 m. Each trial started with a blank screen at second 0. At second 2, a fixation cross was presented at the center of the monitor until the end of the trial at second 7. Simultaneously, a short warning tone occurred at second 2. At second 3, an arrow, pointing either to the left, right, up, or down representing one of four different motor imagery tasks (left hand, right hand, both feet, and tongue, respectively), appeared on the screen for 1.25 s. The period between trials varied randomly between 0.5 and 2.5 s (Fig. 1, right). The subjects were instructed to perform the indicated motor imagery task up to second 7. During the motor imagery task, in particular, the subjects should imagine the indicated movement. They were asked to imagine the (kinesthetic) experience of movement (rather than a visual type of imagery) while remaining relaxed and avoiding any motion during performance. The experiment was divided into 6 runs, consisting of 40 trials each, which led to 60 repetitions of each type of mental task. There were breaks of 3 to 5 min between the runs. Within each run, the tasks were performed in a random order to avoid adaptation.

EEG signals were recorded from a grid of 60 Ag/AgCl scalp electrodes (using a cap by Easycap, Germany) referenced to the left mastoid. The right mastoid electrode served as ground (Fig. 1, left). The closely spaced electrodes with distances of approximately 2.5 cm were placed in a configuration including the electrode positions C3, C4, Cz, Fz, and Pz of the international 10–20 system. The signals were acquired with a SynAmps amplifier (NeuroScan, USA) filtered between 1 and 50 Hz. An additional 50-Hz notch filter was used. The data, including a rectangular trigger signal, were sampled at 250 Hz.

To obtain reference-free EEG data, calculation of source derivation based on the center and the four nearest neighboring electrodes was performed (Hjorth, 1975)—for boundary electrodes, an equivalent calculation was carried out based on the first, second, or third nearest neighbors.

After triggering the data, trials of 10-s length were obtained including 2 s before the warning tone. Single trials were visually inspected for muscle and ocular artifacts, using the software package g.BSanalyze (Guger Technologies, Graz, Austria). Trials containing artifacts were eliminated.

Quantification of ERD/ERS

The quantification of ERD/ERS was carried out in four steps: bandpass filtering of each trial, squaring of samples, and subsequent averaging over trials and over sample points. The ERD/ERS was expressed as percentage power decrease (ERD) or power increase (ERS) in relation to a 1-s reference interval before the warning tone (Pfurtscheller and Lopes da Silva, 1999). The statistical significance of the ERD/ERS values was verified by applying a t percentile bootstrap statistic to calculate confidence intervals with a significance level of $\alpha = 0.05$. This procedure was carried out for overlapping (by 1 Hz) 2-Hz bands in the frequency range between 6 and 42 Hz (for details, see Graimann et al., 2002). The time–frequency maps obtained were used for selection of the alpha (mu) band rhythms with the most significant band power increase or decrease during the motor imagery tasks at the central electrode positions C3, Cz, and C4.

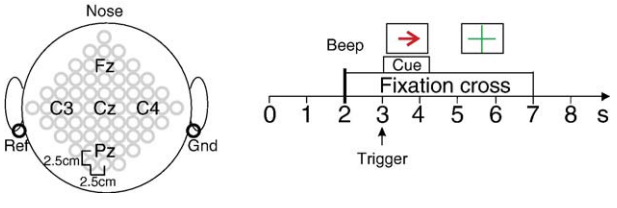

Fig. 1. Electrode positions (left) and experimental paradigm (right).

Analysis and classification of single-trial EEG data

First, the monopolar (raw) EEG data was downsampled from 250 Hz to 125 Hz. Next, adaptive autoregressive (AAR) parameters (of order 3) were estimated for every monopolar channel ($N = 60$) and for every possible combination of bipolar channels ($N = 1770$). Accordingly, 60 + 1770 = 1830 single channel AAR estimates were obtained using the Kalman filtering algorithm (for details, see Schlögl, 2000). Next, the AAR estimates from each trial were divided into segments of 25 samples, i.e., 0.2 s. For each segment, a minimum Mahalanobis distance (MDA) classifier across all trials was calculated and applied to the same segment. This classifier is based on the so-called Mahalanobis distance $d_c(x)$, which is defined as:

$$d_c^2(x) = (x - \mu_c)\Sigma_c^{-1}(x - \mu_c)^T.$$

Here, μ_c is the mean and Σ_c the covariance of the normally distributed class c, estimated from the corresponding training samples. For each testing point x in the n-dimensional feature space, a distance to each class can be calculated, and x is then assigned to the class with the smallest distance. That way, a simple and robust statistical classifier can be obtained which is also applicable to more than two classes.

Accordingly, an average measure for the classification accuracy of the four class problem (four motor imagery tasks) for each segment was obtained. As a measure of distinctiveness, the kappa coefficient κ (Kraemer, 1982) was used. In an M class classification problem, the proper evaluation of the classifier is described by its confusion matrix defining the relationship between the true classes and the output of the classifier. From the confusion matrix H, we can derive the classification accuracy ACC (overall agreement) as follows:

$$ACC = p_0 = \frac{1}{N}\sum_i H_{ii}$$

The chance expected agreement is

$$p_e = \frac{\sum_i n_{oi} n_{io}}{NN},$$

where $N = \sum_i \sum_j H_{ij}$ is the total number of samples, H_{ij} are elements of the confusion matrix H on the main diagonal, and n_{oi} and n_{io} are the sums of each column and each row, respectively. Then the estimate of the kappa coefficient κ is

$$\kappa = \frac{p_0 - p_e}{1 - p_e}$$

with chance probability $p_e = 1/M$. For more details, see also Cohen (1960), Bortz and Lienert (1998) and Kraemer (1982). To compute the kappa coefficient, we used the implementation realized in the BioSig toolbox (Schlögl, 2004).

Within the trial length of 0 to 7s, the 0.2-s segment with the largest κ was used to set up the classifier. The classifier was cross-validated using a leave-one-out approach. This provides 7-s time courses of κ for each of the 1830 channels. Next, for each electrode, the 60 time courses of κ (59 bipolar channels plus 1 monopolar channel) were averaged. The maximum of κ within each averaged time course and electrode is displayed in form of a topographic map (see Fig. 2c).

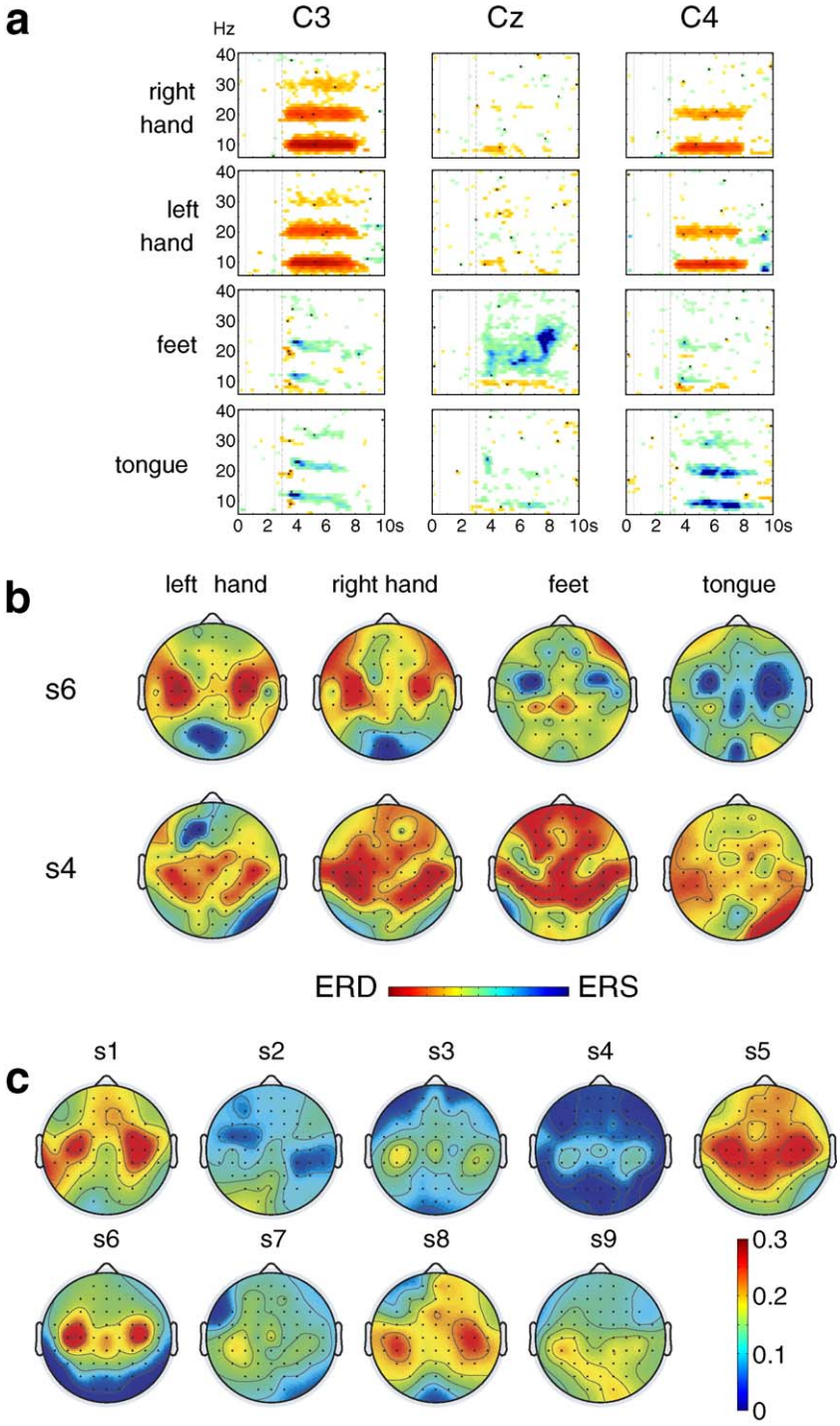

Fig. 2. (a) Examples of time–frequency maps displaying significant ERD (red) and ERS (blue) for one subject (s6), 4 motor imagery task, and 3 electrode locations. (b) Maps displaying the topographical distribution of averaged band power (ERD, ERS) in the upper alpha band (10 to 12 Hz) during 4 motor imagery tasks (second 5.5 to 5.75 of the trial). Data are displayed from 2 representative subjects (s6 and s4, see Table 1). "Red" indicates ERD and "blue" ERS. (c) Topographic maps of averaged kappa maxima. The maps display the topographic distribution of κ for all investigated subjects, based on single-trial classification and discrimination between 4 motor imagery tasks (0 means no and 1 best distinctiveness between motor imagery tasks). The most important locations (electrode positions) are marked by red color.

Results

Averaged band power in alpha (mu) frequency bands during motor imagery tasks

Examples of time–frequency ERD/ERS maps from one subject are presented in Fig. 2a. The maps for electrode positions C3, Cz, and C4 show characteristic patterns of mu and beta ERD only for right and left hand motor imagery, namely, a broad-banded ERD in the 10-Hz and 20-Hz bands at electrode positions C3 and C4 with a contralateral dominance during right hand imagery. Quite different patterns are found with foot and tongue motor imagery. In the first case, an ERS in the 15-Hz band is dominant at Cz, followed by a short-lasting beta burst with frequencies around 25 Hz. In addition, a weak but significant 9-Hz ERD exists over Cz. In the latter case (tongue motor imagery), enhanced narrow-banded 11-Hz, 22-Hz, and 33-Hz components (ERS) are present at electrode position C3. While hand motor imagery blocked or desynchronized the broad-banded mu components, tongue motor imagery enhanced the narrow-banded components. Both low- and high-frequency mu components showed an arch-shaped form as documented by the harmonics in the spectral reactivity patterns. In Fig. 2a, another interesting detail should also be mentioned, namely, that the enhanced mu rhythm during tongue motor imagery had a slightly lower frequency in the right hemisphere as compared to the left hemisphere. This serves as a good example for the independency of the mu generating systems in both hemispheres as already postulated by Storm van Leeuwen et al. (1978).

Table 1 presents the averaged results of band power changes (ERD, ERS) of the most reactive mu components (mean frequencies are indicated) for 3 electrode positions (C3, Cz, C4) and 4 motor imagery tasks (left hand, right hand, foot, tongue). The data show that hand motor imagery induced in a significant mu ERD in all subjects, whereas foot and/or tongue motor imagery revealed a significant ERS in a number of subjects only. The most reactive frequency components varied between 9 and 14 Hz and are found at all central electrode positions and motor tasks. The subjects' individual frequencies varied between 10 Hz ± 1.0 (mean ± SD) and 12 Hz ± 1.1 with a mean of 11.7 Hz ± 0.4 (Table 2).

The discrimination of the frequencies between ERD and ERS revealed a mean frequency of the desynchronized components of 10.9 Hz ± 0.9 and a corresponding frequency of the synchronized components of 12.0 Hz ± 1.0. This difference was significant (t test, $P < 0.05$). Furthermore, the ERD affects more broad-banded components within the alpha band, whereas the ERS enhances narrow-banded components in the upper alpha/lower beta band focused around 12/13 Hz.

From all ERD/ERS values (3 electrodes, 4 tasks) obtained in one subject, the standard deviation was calculated and termed "intertask variability" (ITV). The ITVs presented in Table 2 display low (e.g., subject s4) and high levels (e.g., subject s6). A low ITV indicates an ERD on all central electrode positions during all motor tasks (examples of the individual maps are displayed in Fig. 2b, lower row). In the case of a high ITV, the ERD is dominant only during hand motor imagery, whereas ERS is frequently found during foot and/or tongue motor imagery (examples of maps Fig. 2b, upper row). The obvious difference between foot and tongue motor imagery maps in subject s6 (Fig. 2a) is the midcentral ERD with foot motor imagery and midcentral ERS with tongue motor imagery.

Table 1
Frequencies and band power changes of the most reactive bands displaying ERD/ERS measured at 3 electrode positions and 4 motor tasks

	Left hand						Right hand						Foot						Tongue					
	C3		Cz		C4		C3		Cz		C4		C3		Cz		C4		C3		Cz		C4	
	%	Hz	%	Hz	%	Hz	%	Hz	%	Hz	%	Hz	%	Hz	%	Hz	%	Hz	%	Hz	%	Hz	%	Hz
s1	–83	9	–53	9	–96	11	–95	11	–59	9	–79	12	133	11	–44	11	191	11	151	12	174	11	208	11
s2	–61	11	–50	10	–64	11	–72	11	–27	11	–66	10	–36	13	–30	11	–56	9	–63	9	107	11	–70	9
s3	–28	11	–65	11	–83	13	–64	12	–61	11	–25	11	–27	11	–58	11	195	14	243	13	102	13	191	13
s4	–83	11	–65	11	–88	11	–90	12	–66	11	–82	11	–28	11	–61	11	–67	12	–70	10	–36	13	–76	9
s5	–95	10	–78	9	–93	9	–93	10	–81	10	–83	10	224	14	–80	10	260	14	173	14	120	12	338	14
s6	–95	11	–41	11	–90	11	–97	11	–54	10	–88	11	142	13	–48	10	92	12	238	13	77	11	300	10
s7	–50	11	–36	10	–87	12	–98	12	–62	11	–72	12	–21	11	–53	11	–68	11	179	13	81	13	–54	11
s8	–38	11	–75	9	–86	11	–99	10	–81	9	–79	9	245	10	91	11	212	11	297	12	194	11	218	11
s9	–48	11	–48	11	–93	11	–54	11	–34	10	–70	12	172	11	91	11	255	11	159	11	144	10	147	10
Mean	–64.6	10.7	–56.8	10.1	–86.7	11.1	–84.7	11.1	–58.3	10.2	–71.6	10.9	89.3	11.7	–21.3	10.8	112.7	11.7	145.2	11.9	107.0	11.7	133.6	10.9
SD	25.2	0.7	14.7	0.9	9.4	1.1	16.8	0.8	18.4	0.8	18.8	1.1	116.8	1.3	65.1	0.4	140.8	1.6	128.9	1.6	66.8	1.1	160.5	1.7

Displayed are data from individual subjects. Gray cells indicate ERD, white ones ERS.

Table 2
Mean and intertask variability (ITV) of averaged ERD/ERS values, maximum κ obtained from single-trial classification and mean (median) frequency of the reactive mu components of the 9 subjects investigated

	ERDS			Frequency				
	Mean	ITV	κ	Mean	SD	Min	Max	Med
s1	29	127.93	0.478	10.67	1.07	9.00	12.00	11.00
s2	−40.67	48.98	0.394	10.50	1.17	9.00	13.00	11.00
s3	26.67	120.55	0.367	12.00	1.13	11.00	14.00	11.50
s4	−67.67	19.21	0.298	11.08	1.00	9.00	13.00	11.00
s5	42.67	167	0.482	11.33	2.10	9.00	14.00	10.00
s6	28	139.14	0.501	11.17	1.03	10.00	13.00	11.00
s7	29	127.93	0.478	10.67	1.07	9.00	12.00	11.00
s8	−40.67	48.98	0.394	10.50	1.17	9.00	13.00	11.00
s9	26.67	120.55	0.367	12.00	1.13	11.00	14.00	11.50

Single-trial classification and motor imagery task discrimination

Fig. 2c gives an overview of the topographical distribution of the revealed locations for the discrimination between four motor imagery tasks. The maps show a linear interpolation of the classification accuracy (expressed as maximum of the averaged κ) for the individual subjects. The maps show that the electrode position overlaying approximately the hand representation area (electrode positions C3 and C4) provide the best results of single-trial discrimination between the different motor tasks in the majority of subjects. This is expected because two of the tasks were hand motor imagery, and imagination of hand movement affects mu rhythms in a similar way as observed during execution of the same movement. Interestingly, in some subjects (e.g., subject s6) also, the midcentral electrode position (around Cz) contributed to the best discrimination between the four different motor tasks.

Relationship between intertask variability of mu power changes and single-trial classification accuracy

Fig. 3 displays the relationship between the intertask variability (ITV) and the single-trial classification accuracy of the best performing channel expressed by κ (Table 2) and shows that the power of single-trial discrimination between four different motor tasks increases when central mu rhythms are synchronized and express ERS during foot and/or tongue motor imagery. This is not surprising because it would be nearly impossible to discriminate between four motor imagery tasks if every task displayed very similar centrally localized ERD patterns.

Discussion

"Focal ERD/surround ERS" induced by motor imagery

Basically, hand motor imagery activates neural networks in the cortical hand representation area which is manifested as blocking or desynchronization of the hand area mu rhythm (mu ERD). Such a mu ERD was found in all subjects during right and left hand motor imagery with a clear contralateral dominance. Less clear is the activation of the foot representation area during foot motor imagery because of its location in the mesial wall. In this case, a midcentral mu ERD was found not in all but in the majority of subjects. However, it is very interesting that foot as well as tongue motor imagery enhanced the hand area mu rhythm (mu ERS) in the majority of subjects. This simultaneous pattern of ERD and ERS serves as a good example for the so-called "focal ERD/surround ERS" phenomenon, which describes the observation that desynchronization of alpha (mu) rhythm occurs not in isolation but can be accompanied by an increase in synchronization in neighboring cortical areas that correspond to the same or to another modality (Pfurtscheller and Lopes da Silva, 1999; Suffczynski et al., 2001).

Based on our results on the different center frequencies of the broad-banded ERD (10.9 Hz ± 0.9) and narrow-banded ERS (12.0 Hz ± 1) and the functional dissociation between lower and upper mu rhythms during hand and foot movement execution (Pfurtscheller et al., 2000), the following explanation is suggested: execution and imagination of movement desynchronize lower mu components somatotopically unspecific (similar in hand and foot representation areas) and upper mu components somatotopically specific. In the former case, desynchronization is present in all sensorimotor areas (in target attended and non-attended body part areas), whereas in the latter case of local desynchronization in the attended body part area can be accompanied by a synchronization in non-attended or surrounding areas.

We hypothesize that the enhanced narrow-banded hand area mu rhythm represents a deactivated or inhibited state of hand cortical area networks. In this respect, it is also of interest that the 10-Hz somatosensory (mu) rhythm is also found in magnetoencephalographic (MEG) recordings and interpreted as rhythm characteristic when a sensory cortical area passed into an "idling" state (Salmelin and Hari, 1994, Salmelin et al., 1995). Such inhibition (or passing into an "idling" state of the hand area networks) can occur when the motor attention is directed to the foot or tongue modalities, and attention is withdrawn from the hand. Support for this interpretation comes from regional blood flow (rCBF) measurements showing a decrease in rCBF in the somatosensory cortical representation area of one body part (e.g., hand area) whenever attention is directed to a distant body part (e.g., foot area) (Drevets et al., 1995). Such an interaction is not only possible between different body parts (intramodal) but also between different modalities. For example, a decrease of rCBF in primary somatosensory areas was observed when the subject attended to

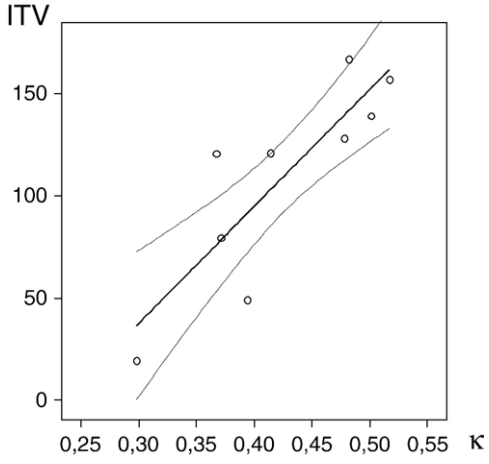

Fig. 3. Relationship between intertask variability (ITV) and single-trial classification accuracy expressed by κ for the 9 able-bodied subjects. A linear regression model was fitted to the data, and in addition, the 95% confidence interval is shown.

a task that involved non-tactile modalities (Kawashima et al., 1995). Further evidence comes from fMRI studies in the visual system showing that attention directed to one stimulus counteracts competitive suppression from multiple visual stimuli in nearby visual space (Kastner et al., 1998).

Relationship between centrally localized ERD/ERS patterns and single-trial classification accuracy

Single-trial classification results indicate that the most important electrode locations for differentiation between different motor imagery tasks are the electrode positions C3, Cz, and C4. This is not unexpected because two of the tasks were hand motor imagery associated with mu ERD at least over the contralateral side (Pfurtscheller et al., 1997), and the two other tasks were foot and tongue motor imagery, respectively, associated with mu ERS in the majority of subjects. It is interesting that different feature extraction and classification methods always document the importance of electrode positions over the hand representation area. Among these are single-trial classification of adaptive autoregressive (AAR) parameters (in our case), the measurement of the proportion of the variance of the mu and/or beta rhythm amplitude that is accounted for by the target location (r^2) (McFarland et al., 1997), and the application of the distinction sensitive learning vector quantification (DSLVQ) (Pregenzer et al., 1996). Also, optimal spatial filtering of multichannel EEG single-trial data revealed electrode positions in the close neighborhood of C3 and C4 as the most important ones for discrimination between different motor imagery tasks (Ramoser et al., 2000). This underlines the importance of the Rolandic mu rhythm, associated with those cortical areas most directly correlated with a motor task for the realization of an EEG-based BCI and the attainment of control over brain oscillations.

Conclusion

During performance of different motor imagery tasks, there exists not only a great intersubject variability but also a considerable intrasubject variability concerning the reactivity of upper mu components. Different types of band power changes (enhancement vs. suppression) during different imagery tasks are a prerequisite for an optimal distinctiveness between different motor imagery tasks when single trials are analyzed. We should emphasize that the ERD/ERS changes reported here were elicited by imagining movements. This implies that such EEG phenomena may be utilized in a brain–computer interface operated simply by motor imagery. Since a number of psychophysiological variables related to perceptual and memory processes and task complexity result in a desynchronization of alpha band rhythms (Klimesch, 1999), it is very difficult to discriminate between more than two mental states when only imagery-induced ERD patterns are available.

Acknowledgments

The work was funded by the European PRESENCIA project (IST-2001-37927) and the Austrian FWF project P16326-BO2. We would like to thank C. Keinrath for the data recording and B. Graimann for the support in signal processing.

References

Bortz, J., Lienert, G.A., 1998. Kurzgefasste Statistik für die klassische Forschung. Springer, Berlin. Kapitel 6: Übereinstimmungsmaße für Subjektive, pp. 265–270.

Brechet, R., Lecasble, R., 1965. Reactivity of mu-rhythm to flicker. Electroencephalogr. Clin. Neurophysiol. 18, 721–722.

Chase, M.H., Harper, R.M., 1971. Somatomotor and visceromotor correlates of operantly conditioned 12–14 Hz sensorimotor cortical activity. Electroencephalogr. Clin. Neurophysiol. 31, 85–92.

Chatrian, G.E., Peterson, M.N.C., Lazarte, J.A., 1959. The blocking of the rolandic wicket rhythm and some central changes related to movement. Electroencephalogr. Clin. Neurophysiol. 11, 497–510.

Cohen, J., 1960. A coefficient of agreement for nominal scales. Educ. Psychol. Meas. 20, 37–46.

Drevets, W.C., Burton, H., Videen, T.O., Snyder, A.Z., Simpson, J.R., Raichle, M.E., 1995. Blood flow changes in human somatosensory cortex during anticipated stimulation. Nature 373, 249–252.

Egner, T., Gruzelier, J.H., 2001. Learned self-regulation of EEG frequency components affects attention and event-related brain potentials in humans. NeuroReport 12 (18), 4155–4159.

Gastaut, H., 1952. Etude electrocorticographique de la reactivite des rhythms rolandiques. Rev. Neurol. 87, 176–182.

Graimann, B., Huggins, J.E., Levine, S.P., Pfurtscheller, G., 2002. Visualization of significant ERD/ERS patterns in multichannel EEG and ECoG data. Clin. Neurophysiol. 113 (1), 43–47.

Hjorth, B., 1975. An on-line transformation of EEG scalp potentials into orthogonal source derivations. Electroencephalogr. Clin. Neurophysiol. 39, 526–530.

Howe, R.C., Sterman, M.B., 1972. Cortical–subcortical EEG correlates of suppressed motor behavior during sleep and waking in the cat. Electroencephalogr. Clin. Neurophysiol. 32, 681–695.

Kastner, S., De Weerd, P., Desimone, R., Ungerleider, L.G., 1998. Mechanisms of directed attention in the human extrastriate cortex as revealed by functional MRI. Science 282, 108–111.

Kawashima, R., O'Sullivan, B.T., Roland, P.E., 1995. Positron-emission tomography studies of cross-modality inhibition in selective attentional tasks: closing the "mind's eye". Proc. Natl. Acad. Sci. U. S. A 92, 5959.

Klimesch, W., 1999. EEG alpha and theta oscillations reflect cognitive and memory performance: a review and analysis. Brain Res. Rev. 29, 169–195.

Koshino, Y., Niedermeyer, E., 1975. Enhancement of rolandic mu rhythm by pattern vision. Electroencephalogr. Clin. Neurophysiol. 38, 535–538.

Kraemer, H.C., 1982. Kappa coefficient. In: Kotz, S., Johnson, N.L. (Eds.), Encyclopedia of Statistical Sciences. John Wiley and Sons, New York.

Lopes da Silva, F.H., 1991. Neural mechanisms underlying brain waves: from neural membranes to networks. Electroencephalogr. Clin. Neurophysiol. 79, 81–93.

McFarland, D.J., McCane, L.M., David, S.V., Wolpaw, J.R., 1997. Spatial filter selection for EEG-based communication. Electroencephalogr. Clin. Neurophysiol. 103, 386–394.

Niedermeyer, E., 1993. The normal EEG of the waking adult. In: Niedermeyer, E., Lopes da Silva, F.H. (Eds.), Electroencephalography: Basic Principles, Clinical Applications and Related Fields. Williams and Wilkins, Baltimore, pp. 131–152.

Pfurtscheller, G., 1992. Event-related synchronization (ERS): an electrophysiological correlate of cortical areas at rest. Electroencephalogr. Clin. Neurophysiol. 83, 62–69.

Pfurtscheller, G., Lopes da Silva, F.H., 1999. Event-related EEG/MEG synchronization and desynchronization: basic principles. Clin. Neurophysiol. 110, 1842–1857.

Pfurtscheller, G., Neuper, C., 1994. Event-related synchronization of mu rhythm in the EEG over the cortical hand area in man. Neurosci. Lett. 174, 93–96.

Pfurtscheller, G., Neuper, C., 1997. Motor imagery activates primary sensorimotor area in humans. Neurosci. Lett. 239, 65–68.

Pfurtscheller, G., Neuper, C., 2001. Motor imagery and direct brain–computer communication. Proc. IEEE 89, 1123–1134.

Pfurtscheller, G., Neuper, C., Flotzinger, D., Pregenzer, M., 1997. EEG-based discrimination between imagination of right and left hand movement. Electroencephalogr. Clin. Neurophysiol. 103, 642–651.

Pfurtscheller, G., Neuper, C., Krausz, G., 2000. Functional dissociation of lower and upper frequency mu rhythms in relation to voluntary limb movement. Clin. Neurophysiol. 111, 1873–1879.

Pregenzer, M., Pfurtscheller, G., Flotzinger, D., 1996. Automated feature selection with a distinction sensitive learning vector quantizer. Neurocomputing 11, 19–29.

Ramoser, H., Müller-Gerking, J., Pfurtscheller, G., 2000. Optimal spatial filtering of single trial EEG during imagined hand movement. IEEE Trans. Rehabil. Eng. 8 (4), 441–446.

Salmelin, R., Hari, R., 1994. Spatiotemporal characteristics of sensorimotor neuromagnetic rhythms related to thumb movement. Neuroscience 60 (2), 537–550.

Salmelin, R., Hämäläinen, M., Kajola, M., Hari, R., 1995. Functional segregation of movement-related rhythmic activity in the human brain. NeuroImage 2, 237–243.

Schlögl, A., 2000. The Electroencephalogram and the Adaptive Autoregressive Model: Theory and Applications. Shaker Verlag, Aachen, Germany.

Schlögl, A., 2004. BioSig-an open source software library for biomedical signal processing. Available online at: http://biosig.sourceforge.net/.

Sterman, M.B., MacDonald, L.R., Stone, R.K., 1974. Biofeedback training of sensorimotor EEG in man and its effects on epilepsy. Epilepsia 15, 395–416.

Storm van Leeuwen, W., Wieneke, G., Spoelstra, P., Versteeg, H., 1978. Lack of bilateral coherence of mu rhythm. Electroencephalogr. Clin. Neurophysiol. 44, 140–146.

Suffczynski, P., Kalitzin, S., Pfurtscheller, G., Lopes da Silva, F.H., 2001. Computational model of thalamo-cortical networks: dynamical control of alpha rhythms in relation to focal attention. Int. J. Psychophysiol. 43, 25–40.

Wolpaw, J.R., Birbaumer, N., McFarland, D.J., Pfurtscheller, G., Vaughan, T.M., 2002. Brain–computer interfaces for communication and control. Clin. Neurophysiol. 113, 767–791.